Fermilab

Fermilab-FN-0954-AD-APC-TD
January 2013

REQUIREMENTS FOR THE MU2E PRODUCTION SOLENOID HEAT AND RADIATION SHIELD*

G. Ambrosio, R. Coleman, V. Kashikhin, M. Lamm, N. Mokhov, J. Popp, V. Pronskikh§

Fermi National Accelerator Laboratory, Batavia IL 60510-5011, USA

Abstract

This paper describes the Heat and Radiation Shield (HRS). It serves to protect the superconducting coils of the Mu2e Production Solenoid (PS) from the intense radiation generated by the 8 GeV kinetic energy primary proton beam striking the production target within the warm bore of the PS. This shield also protects the coils in the far upstream end of the Transport Solenoid (TS), a straight section of coils called TS1, at the exit from the PS. The HRS aperture should allow the maximum stopping rate of negative muons in the Detector Solenoid stopping target. Requirements to the Heat and Radiation Shield are discussed in the paper.

*Work supported by Fermi Research Alliance, LLC under contract No. DE-AC02-07CH11359 with the U.S. Department of Energy.
§ Corresponding author. Email: vspron@fnal.gov

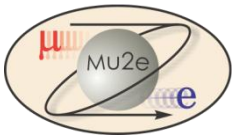

Fermilab

Requirements for the Mu2e Production Solenoid Heat and Radiation Shield

V10

G. Ambrosio, R. Coleman, V. Kashikhin, M. Lamm, N. Mokhov, J. Popp, V. Pronskikh
Mu2e-doc-1092
4/30/2012

Requirements for the Mu2e Production Solenoid Heat and Radiation Shield

This document describes the Heat and Radiation Shield (HRS). It serves to protect the superconducting coils of the Production Solenoid (PS) from the intense radiation generated by the 8 GeV kinetic energy primary proton beam striking the production target within the warm bore of the PS. This shield also protects the coils in the far upstream end of the Transport Solenoid (TS), a straight section of coils called TS1, at the exit from the PS. The HRS aperture should allow the maximum stopping rate of negative muons in the Detector Solenoid stopping target.

There are a number of requirements for the HRS:

1. Production Solenoid Heat and Radiation

   a) Limit the continuous power delivered to the cold mass

   b) Limit the local heat load allowed anywhere within the superconducting coils

   c) Limit the maximum local radiation dose to the superconductor epoxy over the lifetime of the experiment

   d) Limit the damage to the superconductor's Aluminum stabilizer and Copper matrix

2. Production Solenoid field quality should not be degraded by materials used in the HRS

3. Production Solenoid forces during a quench should be minimized by the choice of HRS materials, if possible. The HRS electrical resistivity must be high to limit forces from eddy currents during a quench.

4. Transport Solenoid Heat and Radiation (see #1 above)

5. HRS Thermal Cooling system should limit the temperature on the outer surface of HRS that is in contact with PS cryostat.

6. The HRS must also be adaptable to the design of a remote handling system for the pion production target.

7. Muon Yield should not be reduced significantly by the inner bore size of the HRS.

8. In addition, an acceptable shield design must avoid any line-of-sight cracks between components that point from the target to the inner cryostat wall and thus the magnet coils.

1. Production Solenoid Heat and Radiation

a) Limit the continuous power delivered to the cold mass
An acceptable shield design should establish the following quench limits for nominal operating conditions with the proton beam striking the target: the maximum allowable total heat load for the PS cold mass is 100 W [1].

b) Limit the instantaneous local heat load allowed anywhere within the superconducting coils
A current thermal analysis [1] suggests that the maximum tolerable local heat deposition in the superconductor is 30 micro-watts per gram.

c) Limit the maximum local radiation dose to the superconductor insulation and epoxy over the lifetime of the experiment
In principle, each material included in the construction of the magnet should be rated for the maximum allowable local radiation dose over the operational lifetime of the experiment. In practice, the most radiation-sensitive material sets the lower limit; in particular, the epoxy used to bond the insulation to the superconducting cable can tolerate a maximum of 7 MGy before it experiences a 10% degradation in its shear modulus. The figure below shows some measurements of epoxy damage [2].

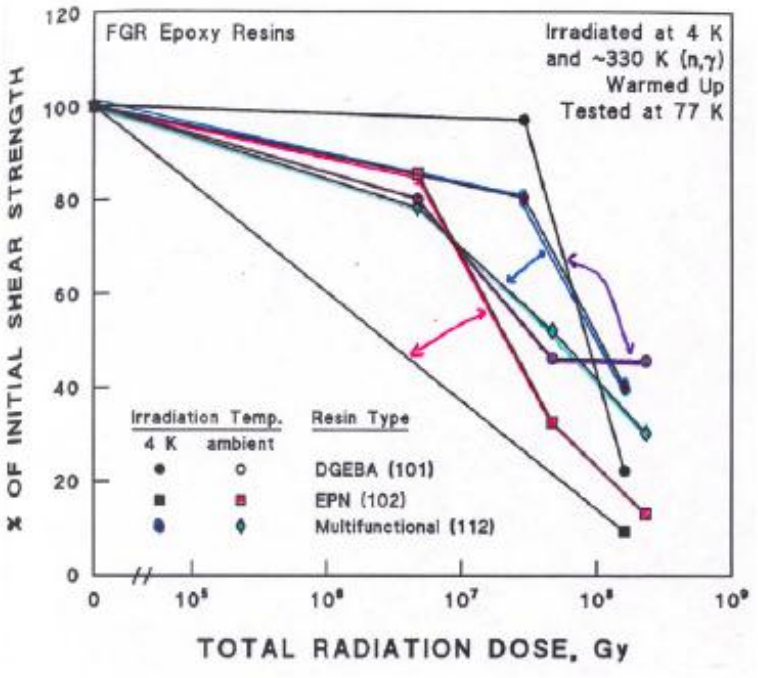

Figure 1.25. A comparison of the shear strengths of three types of reinforced epoxy resins that were reactor-irradiated at both 4 K and at ambient temperature. See text for differences in the fast neutron spectrum in the two reactors. Data from Munshi [1991]. (Supplementary Tables A. 3-3 and A. 8-4.)

Fig 1 Epoxy Radiation Damage

d) Limit the damage to the superconductor's Aluminum stabilizer and Copper Matrix

Introduction

The final parameter describes how radiation affects the electrical conductivity of the component metals of the superconductor cable. At liquid helium temperature, damage to the atomic lattice of a superconducting cable and its quench-stabilizing matrix made from normal conductor takes the form of the accumulation of atomic displacements; i.e., tiny lattice defects. After exposing a metal sample to a given neutron flux spectrum the damage can be characterized by the average number of displacements per atom (DPA). The DPA is directly related to electron transport in metals. The Residual Resistivity Ratio (RRR) is defined as the ratio of the electrical resistance at room temperature of a conductor to that at 4.5 K. For a given sample exposed to various neutron spectra, the RRR will decrease. However, warming such a sample to room temperature leads to recovery of the RRR [3,4], but the degree of recovery depends on the metal. Aluminum is one example material that shows complete recovery, or nearly so, at 300 K. The annealing time was seen to be on a time scale of minutes [4]. This is to be compared to cryogenic heat capacity and expected thermal stresses for the PS during warm-up or cool-down; each would be of order days.

The effect of RRR on the magnet performance

RRR is an important parameter for the superconducting magnet design that affects the magnet performance during operation in superconducting mode and irreversible transition to the normal state (quench). The following list summarizes the most important areas of the magnet performance affected by the RRR:

- *Magnet stability* is the ability of coils to recover the superconducting state after a brief transition into the normal state without the quench. The superconductor transition to the normal state occurs when either the magnetic field, temperature or current exceed the critical values. It can happen for a number of reasons, including rapid heat releases due to cracks in epoxy, slip-stick motion of turns and coils, temperature fluctuation in the cooling system, voltage spikes in the powering circuit and the primary beam mis-steering into the cold mass. While some of the perturbations can be minimized, most cannot be eliminated, and it is therefore safe to assume that a critical perturbation can happen at any given moment during the magnet operation. When it happens, the electric current flowing in the superconductor is forced into the surrounding Cu and Al stabilizers that have much lower resistivity than the superconductor in normal state. The stabilizer resistivity is sufficiently low (i.e. the RRR is sufficiently high) when the resistive heating power of current flowing in the stabilizer is lower than the cooling power due to the heat transfer into the surrounding media. In that case, the temperature returns to the operating temperature after a brief excursion during the critical perturbation. In the opposite case, the normal zone propagates throughout

the coil and eventually all turns transit to the normal state that constitutes the quench.

- *Quench protection* is protection of the magnet during quench from overheating and overvoltage. The resistive heating power of current flowing in the stabilizer during quench is proportional to the stabilizer's resistivity. Therefore, the peak coil temperature during quench is directly affected by the RRR. If the RRR is not sufficiently high, the peak temperature can exceed the maximum acceptable value that is chosen to limit the thermal stresses due to the temperature gradient in the coil. In that case, the thermal stresses can cause damage to the cable or ground insulation.
- *Cooling* during normal operation. The particle radiation deposits a considerable amount of heat in the superconducting coils. In order for the magnet to operate reliably, the coil temperature must be kept below the critical value with a sufficient thermal margin. It is achieved by a system of thermal bridges connecting all turns to the cooling system. For structural reasons, the thermal bridges are made from Al with the same chemical composition as the cable stabilizer. Therefore, it is reasonable to assume that the same degree of radiation damage occurs in the thermal bridges as it does in the cable stabilizer. The ability of the thermal bridges to conduct the heat depends on the thermal conductivity that, according to Wiedemann–Franz law, has the same mechanism as the electric resistivity. Thus it is directly affected by the value of RRR.

The final magnet design will be optimized to work at the minimum RRR of 100 for aluminum and 50 for copper set forth in the PS Requirements Document [5] with sufficient operating margins. However, these margins, governed by the practices applicable to the design of superconducting magnets, do not account for the errors in determining DPA and RRR. Therefore, it is important that the HRS design requirement includes an appropriate safety margin in the maximum acceptable value of DPA to account for these errors, in order to guarantee meeting the minimum RRR requirements with 5 % accuracy.

Measurements of RRR degradation of Aluminum and Copper with radiation

The COMET group from KEK has begun a series of measurements at the Kyoto University Research Reactor. In 2010 they irradiated a sample of Aluminum to a large flux of neutrons at low temperature [6]. The results are shown below for the increase in resistance vs integrated neutron flux.

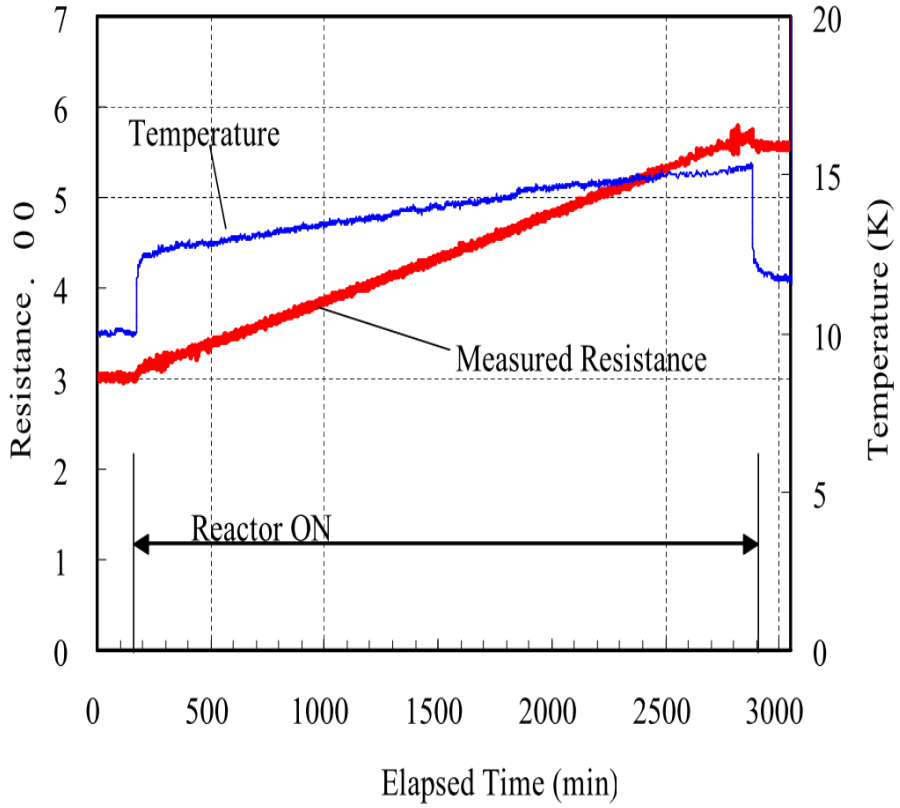

Fig 2 COMET/KEK Measurement

The starting resistance 3.0 μΩ increased to 5.6 μΩ after neutron exposure. The initial resistance before cooldown was 1.37 mΩ. The integrated neutron flux is 2.3 E16 neutrons/cm2 [7]. This is the measurement we currently use for the Mu2e projections. Also importantly for Mu2e, this group observed complete recovery of the Aluminum samples when the temperature rose to room temperature. This recovery of Al is consistent with prior measurements [3,4]. For Cu the recovery of resistivity with annealing is only ~90%.

Some of the other measurements available on Aluminum damage from neutron irradiation at 4 K are summarized in the table below. This compilation is taken from Ref [8] that re-analyzes the experiments with modern theory and consistent parameters. The last column shows the overall adjustment (efficiency η) between analyzed measurements and NRT that varies from 0.357 to 0.535. We will use this range to estimate the uncertainty on our DPA calculation.

Table 1 Summary of Measurements

Measurement	Energy [MeV] or Source	Flux {1E16} Per cm2	$\Delta\rho$ [nΩ-cm]	$\Delta\rho$/Flux [nΩ/cm]	$<\sigma T_d>$ [b*keV]	$\eta = N_D/N_{NRT}$
CP-5(VT53) ANL Kirk et al, Horak 1979 [3,12]	fission ~0.1-7.0	200	382	1.5	76.2	0.357
FISS,FRAGM CP-5 ANL Birtcher et al 1977 [12,13]	fission			57.6	2492.	0.422
LTIF, ORNL Coltman,Klabunde 1982 [15,14,16]	fission	12.3		2.19	98.55	0.405
RTNS,LLL Guinan et al 1982 [16]	14-15	8.2	33.6	4.18	156.9	0.486
LHTL,JPR-3 Takamura et al 1985 [17]	fission	4-12		2.2	81.0	0.495
TTB(1),FRM Wallner et al 1987 [18]	reactor	830	798	2.57	87.6	0.535
COMET/KEK Yoshida et al [7,8]	reactor	2.3 >.1 MeV	5.1	2.2		

Fig 3 Neutron Energy Spectrum for Experiments Prior to COM

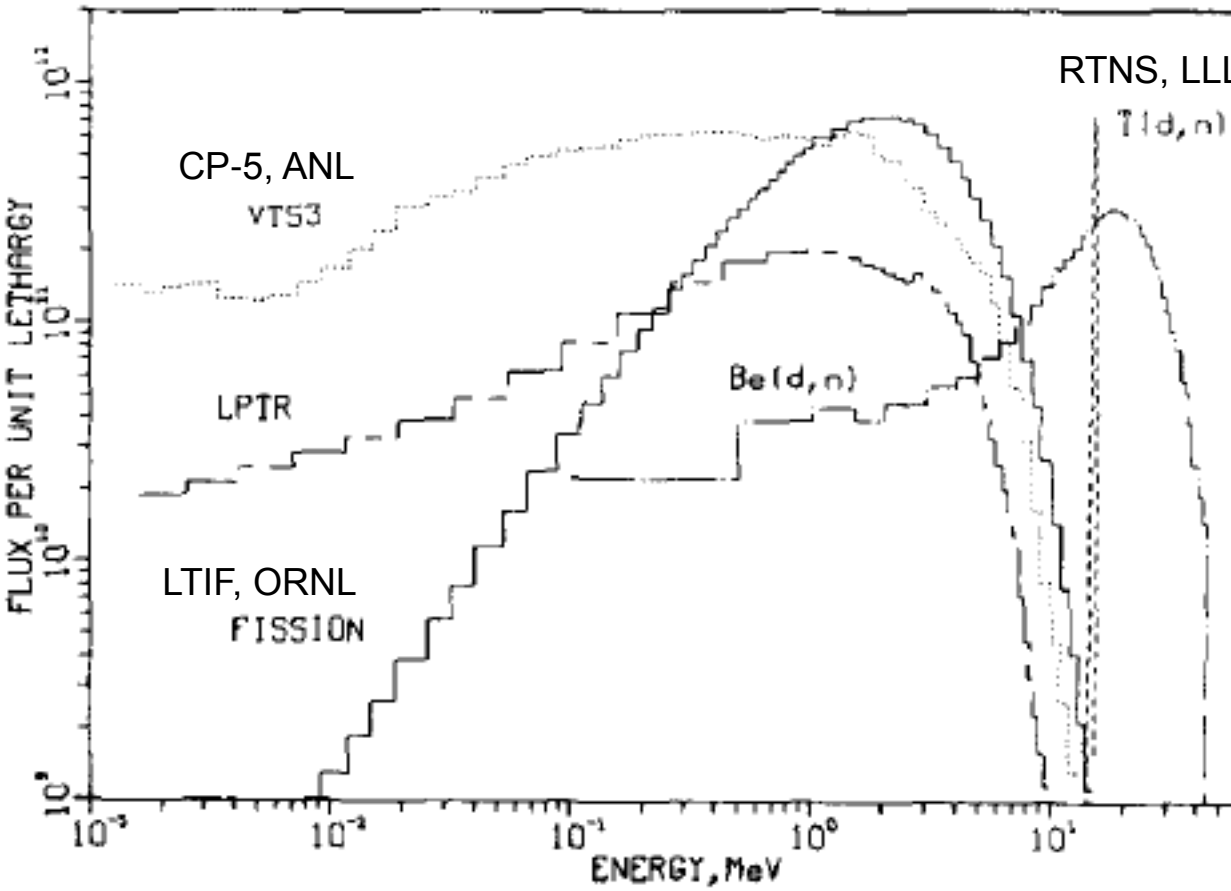

Fig 4 KEK/COMET neutron spectrum compared with other neutron measurements

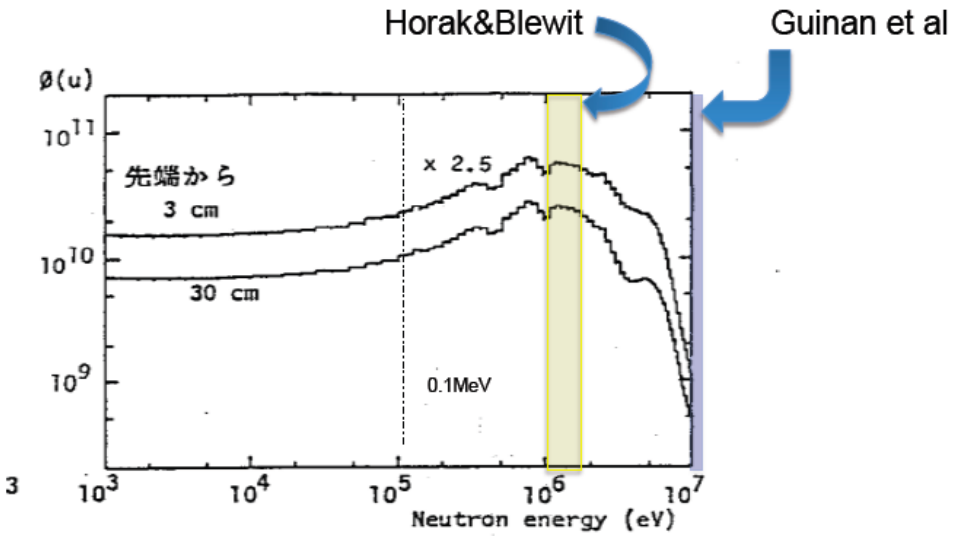

Fig. 15 Neutron energy spectrum in LTL of KUR for ordinary core (above 1000 eV)

KUR-TR287 (1987)

Calculation of DPA for the KEK measurement

Since the KEK measurement was done with a different neutron energy spectrum than Mu2e, a calculation of DPA is need to relate to Mu2e. The model for DPA uses the cross section shown below vs neutron energy in eV [9].

Fig 5

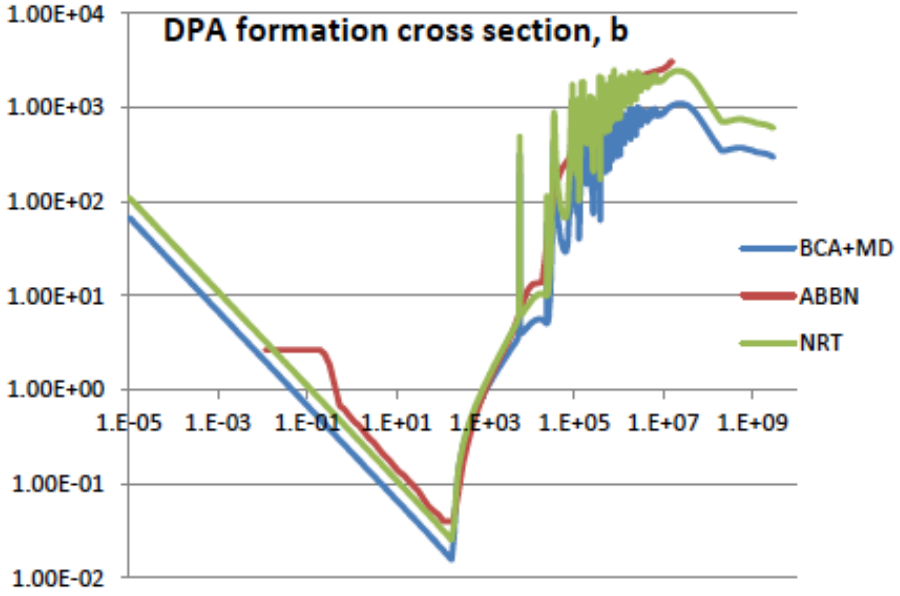

The BCA+MD and NRT models are described in EVAL in Ref [10]. The ABBN model is described in Ref [11].

A comparison of these models with DPA damage from protons on Copper and Tungsten is shown below. While the BCA+MD model agrees better with the data at 1 GeV, in the lower energy region important for Mu2e, the data cannot distinguish the models.

Fig 6 DPA for p + Cu vs Energy

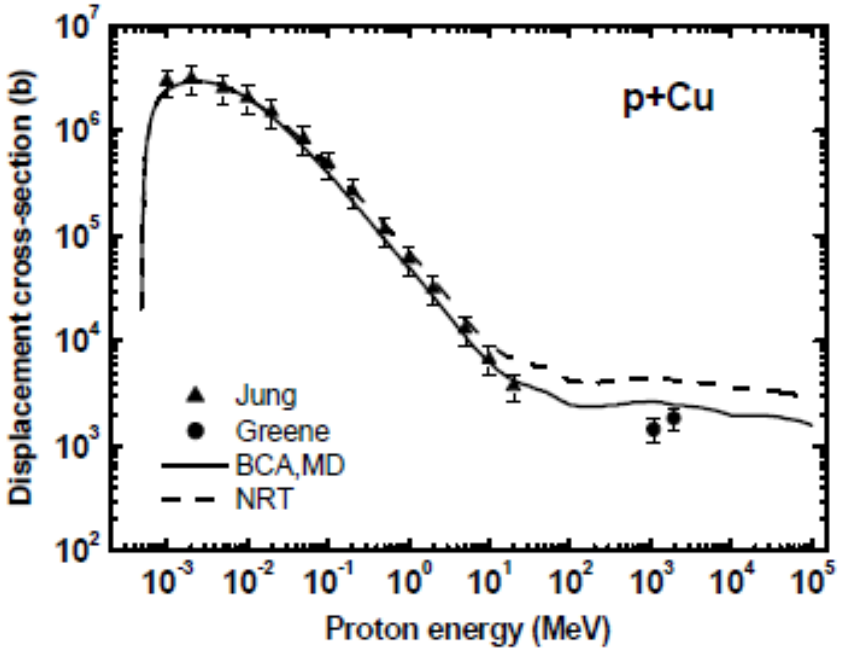

Fig 7 DPA for p+W vs Energy

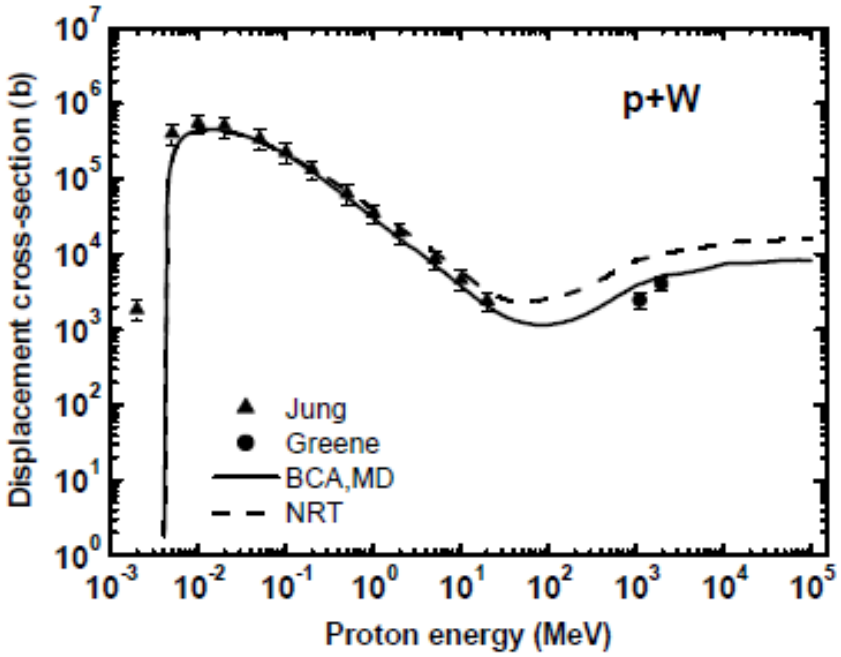

Folding the DPA cross sections with the KEK neutron energy spectrum gives:

Table 2

DPA model	DPA calculated for KEK measurement
BCA+MD	1.0 E-5
NRT	2.5 E-5
ABBN	2.6 E-5

We can now use the KEK measurement of the change in resistance of the Al sample along with the Mu2e-allowed RRR reduction of 1000 to 100, to get limits on DPA exposure for Mu2e. The change in resistivty for the KEK experiment is 5.1 nΩ-cm. Dividing by the DPA in the table above gives the change in resisitivity per DPA shown in the figure below.

Fig 8 RRR vs DPA

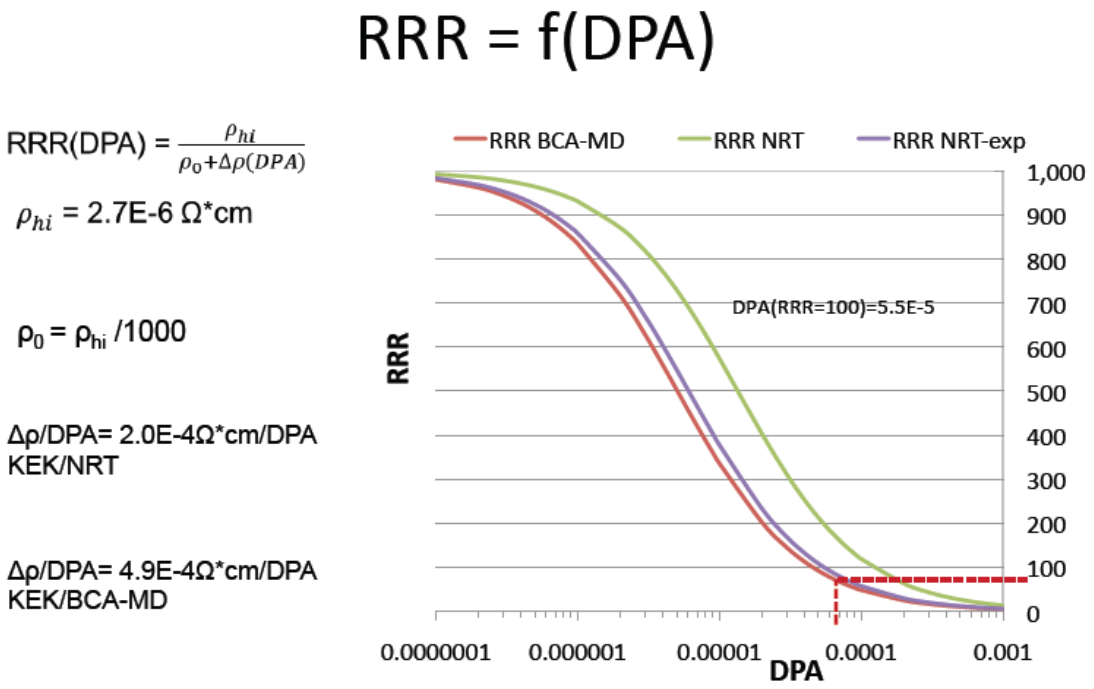

Table 3 Results on DPA for RRR reduction of 1000 to 100 for Mu2e

Measurement/DPA model	DPA [E-5]
BCA+MD	5.0
NRT	12
NRT-exp (using average $\eta = N_D/N_{NRT}$)	5.5

Limit on DPA

The KEK data and the DPA calculation for their neutron spectrum is applied to the Mu2e heat shield and neutron spectrum. We find the reduction in the RRR from 1000 to 100 would require a DPA of 5.5 E-5 using NRT-exp. This amount is allowed in one year of operation, which would be followed by a warm-up to anneal the Aluminum stabilizer. To set a range in the limit, we use the spread in the efficiency $\eta = N_D/N_{NRT} = 0.357$ to 0.535. This gives us a limit of 4 to 6 E-5 for the DPA per year in Mu2e.

2. Production Solenoid Field Quality

The materials used to construct the shield must not cause the magnetic field to fail to meet the required field quality within tolerances, therefore materials with magnetic permeability <1.05 are required [19].

3. Production Solenoid Forces During a Quench

There can be a large axial force on the coils due to eddy currents in the HRS during a quench. Both the choice of materials and construction of the HRS will determine these forces. Higher resistivity materials can reduce these forces (for example bronze C63200 has ~10x higher resistivity than copper). The choice will depend on the trade-off of HRS material and construction cost vs additional coil support [19].

4. Transport Solenoid Heat and Radiation

Two values are tighter than PS requirements for the following reasons: 1) DPA: We want to keep open the option of copper-stabilized cable (instead of Al-stabilized) for possible large cost savings; and 2) Power density: heat extraction from the TS coils is more difficult than from the PS coils because of the smaller cable, the absence of Al-sheets inside the coils, and possible use of copper-stabilized cable.

Therefore the TS DPA requirement is < 1.5 DPA/yr and the power density requirement is <10 uW/g. The total heating should be < 4 watts in TS1 and TS2 [20].

5. HRS Thermal Cooling system should limit the temperature on the outer surface of HRS that is in contact with PS cryostat.

The HRS support rails are the only means of direct heat transfer to the cryostat, since most of the HRS area has a 2.0" clearance. The HRS temperature is not expected to rise too much beyond the cooling water temperature. However we will need to require the HRS water flow to be maintained at all times the magnet is cold and the bore is under vacuum (even if the beam is off) to avoid freezing.

6. The HRS must also be adaptable to the design of a remote handling system for the pion production target[21].

7. Muon Yield should not be reduced significantly by the inner bore size of the HRS.

The inner shield wall is limited to no less than 25 cm [22] since smaller radii negatively impact the stopped muon yield in the Detector Solenoid.

8. In addition, an acceptable shield design must avoid any line-of-sight cracks between components that point from the target to the inner cryostat wall and thus the magnet coils.
Simulations indicated that only cracks larger than a few millimeters are of concern; this should not be a problem.

References:

1. Mu2e Conceptual Design Report (chapter 7), March 2012, Mu2e-docdb-1169.
2. Radiation Hard Coils, A. Zeller et al, 2003, http://supercon.lbl.gov/WAAM
3. Isochronal Recovery of Fast Neutron Irradiated Metals, J. Horak and T. Blewitt, J. Nucl. Mat., 49(1973/74) 161-180.
4. Defect Production and Recovery in FCC Metals Irradiated at 4.2 K, M.Guinan et al, J. Nucl. Mater. 133&134 (1985) 357-360.
5. Mu2e Production Solenoid Requirements Document, M. Lamm & V. Kashikhin, April 2011, Mu2e-docdb-1406.
6. COMET Magnets Design and Radiation Effects, M. Yoshida, Mar. 2011, Mu2e-docdb-1406.
7. M. Yoshida et al, ICMC2011.
8. Development of Calculation Methods to Analyze Radiation Damage, Nuclide Production and Energy Deposition in ADS Materials and Nuclear Data Evaluation, C. Broeders and A. Konobeyev, Aug. 2006, Volume 7197 of Wissenschaftliche Berichte // Forschungszentrum Karlsruhe in der Helmholtz-Gemeinschaft
9. DPA Calculation in the Reactor Neutron Energy Range, V. Pronskikh and N. Mokhov, June 2011, Mu2e-docdb-1851.
10. EVAL-Oct 10 by U. Fischer and A.Yu. Konobeyev
11. S. V. Zabrodskaya et al, IPPE, 1993.
12. M.A. Kirk, L.R. Greenwood, J. Nucl. Mater. 80 (1979) 159.
13. R.C. Birtcher, R.S. Averback, T.H. Blewitt, J. Nucl. Mater.75 (1978) 167.
14. R.R. Coltman, Jr., C.E. Klabunde, J.M. Williams, J. Nucl. Mater. 99 (1981) 284.
15. C.E. Klabunde, R.R. Coltman, J. Nucl. Mater. 108&9 (1982) 183.
16. M.W. Guninan, J.H. Kinney, J. Nucl. Mater. 108&9 (1982) 95.
17. S. Takamura, T. Aruga, K. Nakata, J. Nucl. Mater. 136(1985).
18. Mu2e-docdb-1853
19. Private communication with V. Kashikhin, FNAL.
20. Private communication with G. Ambrosio, FNAL.
21. Second STFC-RAL Conceptual Design Study of Mu2e Experiment Mu2e Pion Production Target Components and Systems, C. J. Densham et al, July 2011, Mu2e-docdb-1746.
22. Comparison of Different Heat Shield Inner Radii, V. Khalatian, April 2011, Mu2e-docdb-1487.

Appendix
Mu2e HRS performance relative to specifications

Fig A1 The original Mu2e Baseline HRS using a combination of Tungsten and Copper

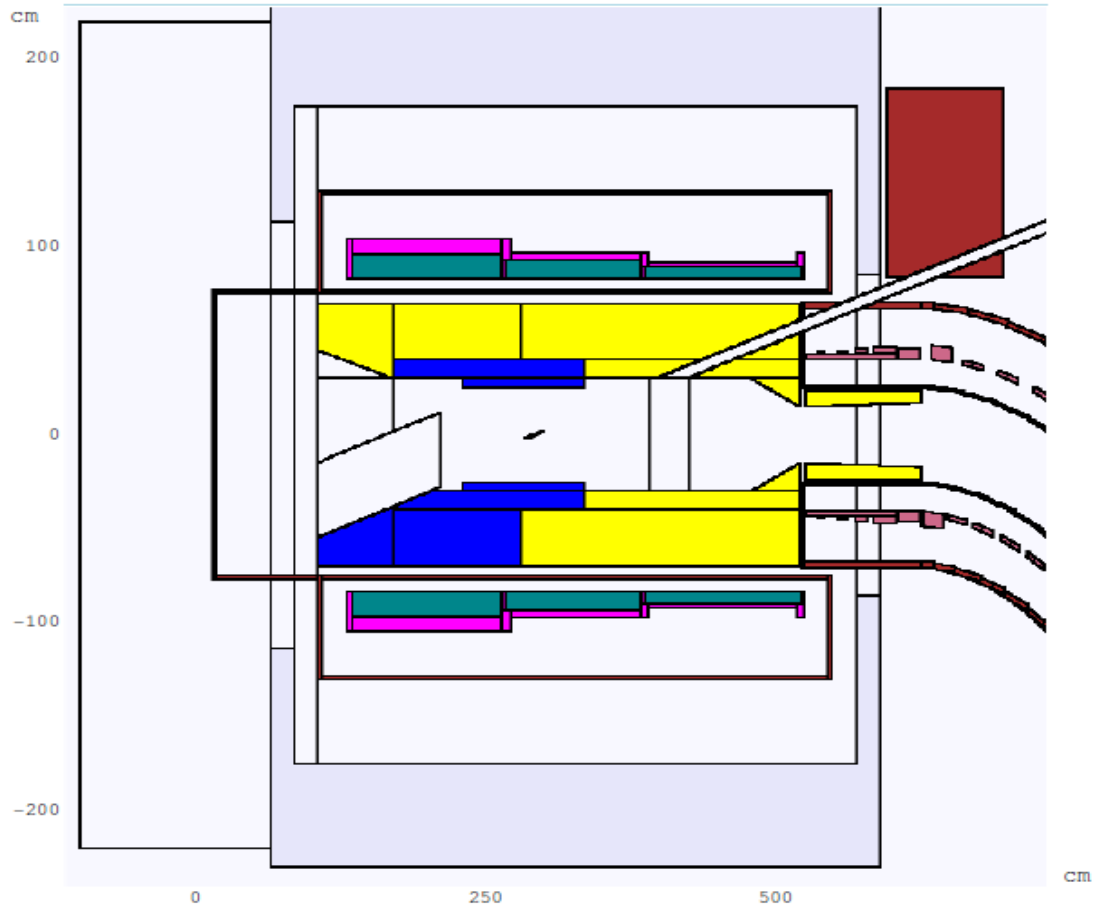

The original baseline shield consists of cylindrical shapes with various cross-sections. The yellow portions are made of copper and the blue of tungsten. The model has an outer radius of 70 cm. A 5 cm radial gap, reserved for additional shielding, exists between this model and the inner wall of the PS cryostat. The entire PS inner cryostat wall, at a radius of 75 cm, will support the final HRS design. The length of the HRS is about 4 m and has a smallest inner radius of 30 cm. The pion production target is located in this cavity, as shown in the figure, and under vacuum. More recently we are considering an all-bronze option to reduce the cost.

All the calculations in this section were done using MARS. The PS calculations for the original baseline consisting of tungsten and bronze are taken from V. Pronskikh [Mu2e-docdb-1849]. The ones for all bronze are from V. Pronskikh and N. Mokhov [Mu2e-docdb-1870]. The bronze here was the preferred high silicon bronze by the magnet team with high electrical resistivity and a density of 8.5 g/cm3. Later we found the only bronze available from vendors in the large forged pieces we wanted was C63200. The calculations were repeated with C63200 bronze with a density of 7.6 g/cm3 and those results are used for the all-bronze HRS given below.

The Mu2e calculated neutron spectrum is shown below. The red curve shows the energy spectrum before the HRS absorber and the blue curve is after the HRS absorber just before the coils. The neutron flux per cm2 per dE [GeV] per proton on target is plotted.

Fig A2 The Mu2e neutron spectrum before (red) and after (blue) the HRS absorber

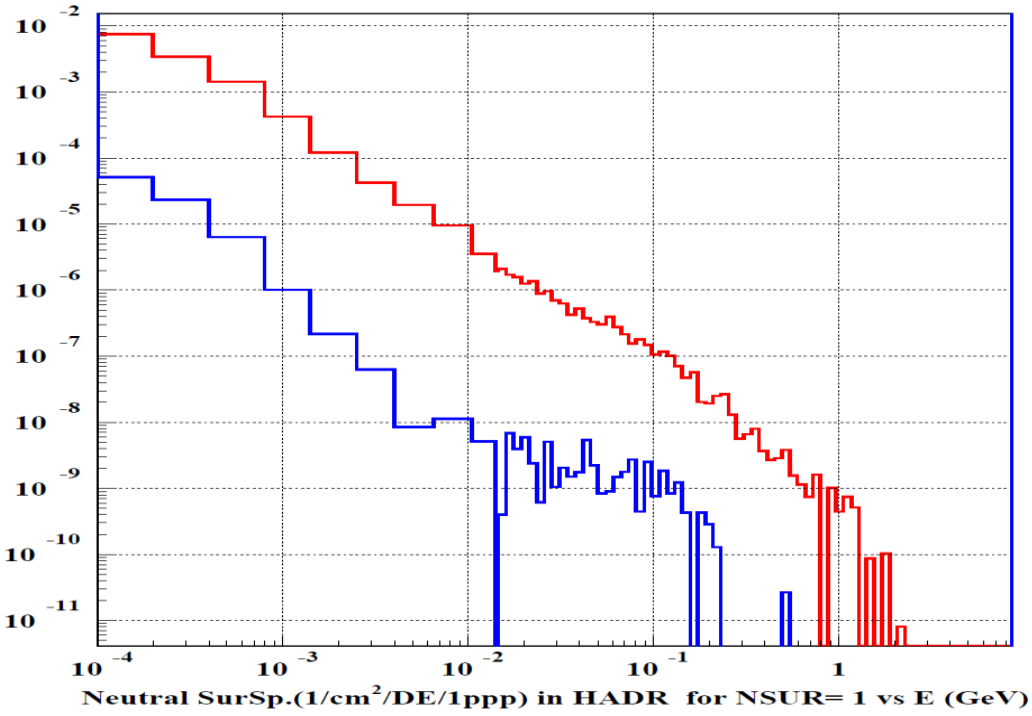

Table A1 Production Solenoid Specifications compared to Simulated Performance

Beam Power (kW)	HRS	Peak DPA/yr [E-5]	Peak Power Density [uW/g]	Rads/yr [MGy/yr]*	Years Before 7 MGy	watts
25	**Specification**	4 to 6	30	0.35	20	100
25	**Simulation W&Bronze Baseline**	2.9	13	0.27	30	53
25	**Simulation all Bronze**	9.6	51	0.99	7	60
8.3	"	3.2	17	0.33	21	20

* This is the DPA damage per year we can get which RRR degrades to 100. After this RRR reduction we must warm-up and anneal.

Table A2 Transport Solenoid Specifications compared to Simulated Performance
Values given for Al and Cu based coils on an Al bobbin[Mu2e-docdb-1850]

Beam Power (kW)	HRS	Peak DPA/yr [E-5]	Peak Power Density [uW/g]	Rads/yr [MGy/yr]*	Years Before 7 MGy	watts
25	**Specification**	1.5	10	0.35	20	4 TS1&2
25	**Design ***	1 (Cu) 1.4 (Al)	7 (Cu) 4 (Al)	0.13 (Cu) 0.13 (Al)		
8.3	"	0.33 (Cu) 0.47 (Al)	2.3(Cu) 1.3 (Al)	0.04(Cu) 0.04 (Al)		

* Results for TS do not depend too much on whether the HRS has partially tungsten or all bronze because both designs are identical near the TS. Here we quote all bronze results.